HHS Public Access

Author manuscript

J Cell Physiol. Author manuscript; available in PMC 2022 February 01.

Published in final edited form as:

J Cell Physiol. 2021 February ; 236(2): 1332–1344. doi:10.1002/jcp.29940.

INCREASED CELLULAR SENESCENCE IN THE MURINE AND HUMAN STENOTIC KIDNEY: EFFECT OF MESENCHYMAL STEM CELLS

Seo Rin Kim, MD[a], **Xiangyu Zou, MD**[a], **Hui Tang, MD**[a], **Amrutesh S. Puranik**[a], **Abdelrhman M. Abumoawad, MD**[a], **Xiang-Yang Zhu, MD**[a], **LaTonya J. Hickson, MD**[a], **Tamara Tchkonia, PhD**[b], **Stephen C. Textor, MD**[a], **James L. Kirkland, MD, PhD**[b], **Lilach O. Lerman, MD, PhD**[a]

[a]Division of Nephrology and Hypertension, Mayo Clinic, Rochester, MN, USA

[b]Robert and Arlene Kogod Center on Aging, Mayo Clinic, Rochester, MN, USA

Abstract

Cell stress may give rise to insuperable growth arrest, which is defined as cellular senescence. Stenotic kidney (STK) ischemia and injury induced by renal artery stenosis (RAS) may be associated with cellular senescence. Mesenchymal stem cells (MSCs) decrease some forms of STK injury, but their ability to reverse senescence in RAS remains unknown. We hypothesized that RAS evokes STK senescence, which would be ameliorated by MSCs. Mice were studied after 4 weeks of RAS, RAS treated with adipose tissue-derived MSCs 2 weeks earlier, or sham. STK senescence-associated β-galactosidase (SA-β-Gal) activity was measured. Protein and gene expression was used to assess senescence and the senescence-associated secretory phenotype (SASP), and staining for renal fibrosis, inflammation, and capillary density. Additionally, senescence was assessed as *p*16+ and *p*21+ urinary exosomes in patients with renovascular hypertension (RVH) without or 3 months after autologous adipose tissue-derived MSC delivery, and in healthy volunteers (HV). In RAS mice, STK SA-β-Gal activity increased, and senescence and SASP marker expression was markedly elevated. MSCs improved renal function, fibrosis, inflammation, and capillary density, and attenuated SA-β-Gal activity, but most senescence and SASP levels remained unchanged. Congruently, in human RVH, *p*21+ urinary exosomes were elevated compared to HV, and only slightly improved by MSC, whereas p16+ exosomes remained unchanged. Therefore, RAS triggers renal senescence in both mice and human subjects. MSCs

Corresponding Author: Lilach O. Lerman, MD, PhD, Division of Nephrology and Hypertension, Mayo Clinic, 200 First St SW, Rochester, MN 55905, Phone: 507-206-9376, Fax: 507-206-9316, Lerman.Lilach@Mayo.edu.

Current addresses of the authors: Seo Rin Kim[1], Xiangyu Zou[2], Amrutesh S. Puranik[3]

[1]Department of Nephrology and Research Institute for Convergence of Biomedical Science and Technology, Pusan National University Yangsan Hospital, Yangsan, Korea, [2]Department of Urology, Xinhua Hospital, Shanghai Jiao Tong University School of Medicine, Shanghai, China, [3]Colton Center for Autoimmunity, Division of Rheumatology, New York University Langone Medical Center, NY, USA

Author contributions

SR.K., X.Y.Z., and L.O.L. designed the study; SR.K., X.Z., H.T., A.M.A., and A.S.P. carried out experiments; SR.K., X.Y.Z., and L.O.L. analyzed the data; SR.K. statistical analysis; X.Y.Z., L.J.H., T.T., S.C.T., J.L.K., and L.O.L. supervision or providing intellectual content of critical importance to the work described; S.C.T., J.L.K., and L.O.L. mentorship; all authors approved the final version of the manuscript.

Data Availability Statement

The data that support the findings of this study are available from the corresponding author upon reasonable request.

decrease renal injury, but only partly mitigate renal senescence. These observations support exploration of targeted senolytic therapy in RAS.

Keywords

cellular senescence; renal artery obstruction; mesenchymal stem cells; exosomes; kidney

Introduction

Cell stress may provoke insuperable growth arrest, which is defined as cellular senescence (Y. Zhu, Armstrong, Tchkonia, & Kirkland, 2014). Senescent cells can have distinctive features, including senescence-associated secretory phenotype (SASP) and senescent-cell anti-apoptotic pathways (SCAP). SASP is a cellular protein secretion profile that can consolidate senescence, exert noxious effects on adjacent cells, and lead to organ dysfunction (Y. Zhu et al., 2014). Senescent cells acquire resistance to apoptosis, termed SCAP, and extend their survival, hence augmenting their ripple effects (Y. Zhu et al., 2015). Cellular senescence is important for suppression of cancer, but has also been implicated as a possible contributor to aging and to the pathogenesis of tissue injury in diseases including hypertension, atherosclerosis, acute kidney injury (Jin et al., 2019), heart failure, and peripheral vascular disease (Y. Zhu et al., 2014). However, the potential involvement of senescence in chronic ischemic kidney injury is unknown.

Severe renal artery stenosis (RAS) induces stenotic kidney (STK) dysfunction by triggering oxidative stress, inflammation, fibrosis, and microvascular loss (Kwon & Lerman, 2015), but the role of cellular senescence has not been fully elucidated. Recently, delivery of adipose tissue-derived mesenchymal stem cells (MSCs) into the STK has been shown to blunt pathophysiological pathways underlying kidney damage, and improve renal function in pig models of RAS (Eirin et al., 2012). This is likely attributable to the potent immunomodulatory properties of MSCs *via* their paracrine anti-inflammatory actions (Biancone, Bruno, Deregibus, Tetta, & Camussi, 2012). In AKI MSCs also protect against premature renal senescence-associated cell-cycle arrest resulting from oxidative stress (Rodrigues et al., 2017). However, under chronic ischemic conditions, persistent senescence and development of SASP might sustain a perpetual state of damage (Chandrasekaran, Idelchik, & Melendez, 2017) that would be harder to reverse without targeted interventions. Thus, it remains unknown if the beneficial effects of MSC in chronic RAS include reversal of senescence.

This study was therefore designed to test the hypothesis that RAS evokes STK senescence and to test whether it can be ameliorated by MSCs.

Concise methods

Mouse model

All animal procedures followed the National Institutes of Health's Guide for the Care and Use of Laboratory Animals and were approved by the Mayo Clinic Institutional Animal Care and Use Committee. Eighteen male 129-S1 mice (Jackson Lab, Bar Harbor, ME, 11

weeks of age) were studied for 4 weeks, after being randomly divided into RAS, RAS +MSC, and sham groups (n=6 each). RAS was induced at baseline by surgical placement of a peri-arterial cuff (n=12) (Ebrahimi et al., 2013), whereas sham surgeries were performed in the control group (n=6). Two weeks after induction of RAS, allogeneic adipose tissue-derived MSCs (5×10^5 cells in 200uL Phosphate-buffered saline) were delivered to the RAS +MSC mice via intra-aortic injection (Eirin et al., 2012). Blood pressure (BP) was measured in all mice weekly by tail-cuff. Four weeks after surgeries, mice were weighed and then euthanized by terminal blood collection (exsanguination). Both kidneys were removed, weighed, and dissected for *ex-vivo* studies, and plasma creatinine level determined. SA-β-Gal staining was performed on renal cryo-sections, and fluorometric SA-β-Gal activity assayed in homogenized kidney tissue (Kim, Eirin, Zhang, Lerman, & Lerman, 2019; Pawar et al., 2019). Real-time PCR was used to assess *p*16, *p*21, *p*53, Activin-A, hypoxia-inducible factor (HIF)-1α, interleukin (IL)-1α, IL-6, and tumor necrosis-factor (TNF)-α gene expression in each homogenized renal samples. Protein expression of p16, p21, p53, activing-A, IL-6, and TNF-α was measured in homogenized kidney tissue by Western blot. To estimate renal fibrosis, Sirius red staining was performed on paraffin sections. Additionally, immunohistochemistry staining against F4/80 and CD31 was performed to evaluate macrophage infiltration and microvascular density, respectively.

MSC preparation.—Allogeneic MSCs were collected from abdominal fat of 129s1 donor mice, digested, filtered, and cultured for 2–3 weeks. Third passage cells were collected and characterized by immunostaining and fluorescence-activated cell sorting analysis to determine cellular phenotype for Sca-1, CD73, CD90, CD34, and CD45 (Ezquer et al., 2016). A MSC functional identification kit was used for assaying tri-lineage differentiation capacity (Eirin et al., 2015). MSCs were labeled prior to delivery with a fluorescent membrane dye. Five additional RAS mice were euthanized 24 hours after MSC injection, to evaluate localization and potential rejection of MSCs in 5μm stenotic kidney sections by immunofluorescence staining with lectin and CD3, respectively (Eirin et al., 2015).

Human RAS

Patient recruitment.—Nondiabetic patients with significant RAS and renovascular hypertension (RVH) (n=13) were prospectively enrolled as a part of another study (Saad et al., 2017). We included patients with hypertension (Systolic blood pressure (SBP) >155mmHg and/or the use of at least two BP drugs) and renal artery Doppler ultrasound velocity acceleration (average peak systolic velocity>300 cm/s). Six additional patients were treated with a single intra-arterial infusion of autologous MSCs (5×10^5 cells/kg) in the renal artery (RVH+MSC group). Age-matched healthy volunteers (HV) (n=13) without cardiovascular risk factors were recruited through the Mayo Clinic Biobank. The Mayo Clinic Institutional Review Board approved this study, conducted in accordance with the ethical principles of the Declaration of Helsinki, and informed consent was obtained.

MSC preparation and delivery.—Autologous human MSCs were harvested from a subcutaneous abdominal fat biopsy sample sterilely obtained six weeks before delivery (Saad et al., 2017). After sterility test using anaerobic and aerobic culture, endotoxin, mycoplasma, karyotype, and FACS for surface markers characteristic of MSC, release for

administration was determined. A 3-day inpatient protocol was performed in patients with RVH as previously described (Saad et al., 2017). All patients were taking angiotensin-converting enzyme inhibitors or angiotensin receptor blockers and continued with this regimen during the study. During the protocol, dietary sodium intake was controlled at 150 mEq/day. BP was measured 3 times daily using automated oscillometric device. Blood and urine samples were obtained on the first day. Estimated glomerular filtration rate (eGFR) was calculated by the Modification of Diet in Renal Disease equation. In RVH+MSC group, standard aortic cannulation was performed via the femoral artery with heparin (4000 U) administration. Then the stenotic renal artery was selectively cannulated, and MSCs in 10 ml of Lactated Ringer's solution manually injected distal to the stenosis over 5 minutes. Blood and urine samples were also studied in RVH+MSC at a 3-month return visit. In HV, blood and urine samples were collected during a single-visit, and dietary sodium intake was not regulated.

Isolation and characterization of urinary exosomes.—Urinary exosomes were isolated using Urine Exosome RNA Isolation Kit on 5ml urine sample (Santelli et al., 2019; Sun et al., 2018). Nanoparticle tracking analysis was performed to assess the concentration and size distribution of the exosomes (Eirin et al., 2017). Total RNA from urinary exosomes was obtained and gene expression of *p*16 and *p*21 determined using quantitative PCR. The percentage of exosomes positive for *p*16 and *p*21 was calculated using imaging flow cytometry (Santelli et al., 2019).

Statistical Analysis

Statistical analysis was performed using JMP software version 13.0 (SAS Institute Inc., Cary, NC). Results are presented as mean±SD for normally distributed variables and as median (interquartile range) for data that did not show a normal distribution. Parametric (one-way analysis of variance (ANOVA) followed by Tukey) and non-parametric (Kruskal-Wallis followed by Steel-Dwass) test were used for comparisons among groups. A $P \leq 0.05$ was considered statistically significant.

Complete and detailed methods are provided as Supplemental Material.

Results

MSC characterization

Flow cytometry showed that MSCs harvested from abdominal adipose tissue of adult male mice expressed the typical stem cell markers Sca-1, CD73, and CD90, but not CD45 and CD34 (Fig. 1A). Moreover, trans-differentiation into chondrocytes, adipocytes, and osteocytes (Fig. 1B) confirmed their mesenchymal lineage. In the kidney, allogeneic MSCs co-localized with tubular lectin (Fig. 1C) but not CD3, arguing against immune rejection (Fig. 1D).

Characteristics of mice

Final body weights of mice with RAS were lower than sham (P=0.01) and tended to be lower than RAS+MSC (P=0.08) (Table 1). After 4 weeks of RAS, the atrophic STK was

markedly smaller than the sham (P<0.0001) and contralateral kidney (CLK) (P<0.0001). In RAS+MSC, STK weight was not different from RAS (P=0.94); the CLK was heavier (P=0.05), but STK/CLK ratio was comparable (P=0.95). Creatinine levels were elevated in RAS compared with both sham (P=0.004) and RAS+MSC (P=0.003). SBP was similar among the groups at baseline (P=0.95), but rose in both RAS groups by 2 weeks after RAS induction (P≤0.05 *vs.* sham and *vs.* baseline) (Fig. 2A). MSCs had no effect on BP (P=0.95 *vs.* RAS).

Renal senescence

On renal cryosections marked positive SA-β-Gal (blue) staining, indicative of senescent cells, was detected in the STK, particularly in cortical tubules and glomeruli (Fig. 2B). Compared to sham kidneys, the STK showed a higher SA-β-Gal+ area (P=0.02) and activity (P=0.03) (Fig. 2C). In RAS+MSC SA-β-Gal staining was not different than RAS (P=0.37), yet was no longer higher than sham, and SA-β-Gal activity decreased (P=0.03). Renal *p*16, *p*21, *p*53, Activin-A, HIF-1α, IL-1α, IL-6, and TNF-α gene expression was markedly (up to 1,000-fold) elevated in the STK compared with sham (all P≤0.01), but showed no change after MSC delivery (P≥0.56 for all *vs.* RAS) with the exception of IL-6, which decreased after MSC delivery (P=0.04 *vs.* RAS), yet was not normalized (Fig. 3A). Renal protein expression of p16, p21, p53, IL-6, and TNF-α relative to GAPDH was also higher in RAS than sham (all P≤0.0005) (Figs. 3B, S1). MSC reduced IL-6 levels (P=0.01 *vs.* RAS), but no other proteins (P≥0.06 for all *vs.* RAS). Activin-A protein level was similar among the groups.

Renal tissue injury

Sirius red staining illustrated that RAS led to increased collagen deposition in the STK compared to sham kidneys (P=0.003), which fell in RAS+MSC (P=0.03 *vs.* RAS, Fig. 4A). STK macrophage infiltration (F4/80 staining) was augmented in RAS and RAS+MSC compared to sham (P<0.0001 and P=0.0008, respectively), but lower in RAS+MSC than in RAS (P=0.002). RAS also showed lower microvascular density (CD31 staining) than sham (P<0.0001), which was restored after MSC treatment (P=0.05). SA-β-Gal positive area correlated directly with renal fibrosis (P<0.0001) and inversely with microvascular density (P=0.002, Fig. 4B).

Human urinary exosomes

At enrollment, peak US Doppler velocity of stenotic renal artery was not different between RVH and RVH+MSC (P=0.76, 405 (302.5–422.5) and 417 (293.5–424.25) cm/s, respectively), suggesting a comparable severity of RAS. We analyzed urinary exosomes from HV and RVH patients with or without MSC injection, whose characteristics are summarized in Table 2. BMI were higher in RVH than HV (P=0.03), but age was not different among the 3 groups. SBP and mean arterial pressure were increased in RVH compared to HV (P<0.001 and P=0.01, respectively), and SBP was lower in RVH+MSC than RVH (P=0.02). Serum creatinine was higher only in RVH than in HV (P=0.01), but eGFR was lower in both RVH and RVH+MSC (P<0.001 and P=0.03, respectively).

Nanoparticle tracking of particles isolated from the urine showed a size distribution mainly between 30–100nm (Fig. 5A), consistent with exosomes. *p*16 gene expression in urinary exosomes was not different among the groups (P=0.1) regardless of adjustment for BMI (P=0.07, Fig. 5B). Contrarily, *p*21 gene expression was elevated in urinary exosomes of patients with RVH compared with HV (P=0.008) and tended to increase in patients with RVH+MSC compared with HV (P=0.09) (Fig. 5C). After adjustment for BMI, *p*21 gene expression remained higher in patients with RVH than HV (P=0.03) and was not different between RVH and RVH+MSC (P=0.33), or between HV and RVH+MSC (P=0.28). Imaging flow cytometry showed increased percentage of p21+ urinary exosomes in RVH compared to HV (P=0.0003), which was not different in RVH+MSC compared to either HV (P=0.15) of RVH (P=0.17) (Fig. 6). Urinary p16+ urinary exosomes were comparable among the groups (Fig. 6).

Discussion

The current study shows that renal senescence markers, including SA-β-gal and senescence-associated gene expression, were markedly elevated in the murine STK, implicating cellular senescence in the pathogenesis of chronic ischemic renal injury. This is further supported by the expression of SASP indices, such as IL-1α, IL-6, and TNF-α, which was significantly upregulated in the STK. Comparably, renal senescence signals were evident in urinary exosomes of patients with RVH. In the murine model, MSC treatment improved renal function, fibrosis, inflammation, and capillary density, and decreased SA-β-Gal activity and IL-6 overexpression, but other key senescent markers remained unaltered after MSC delivery. Similarly, MSC only partly improved p21 expression in urinary exosomes of human subjects with RVH. This implies that MSC therapy only partly mitigates cell-cycle arrest associated with renal senescence activity in chronic renal ischemia, yet blunts some downstream or alternative pathways leading to renal damage. Taken together, these observations support exploration of targeted senolytic therapy in RAS.

Markers of cellular senescence have been detected in renal aging and disease processes including acute kidney injury, diabetic nephropathy, glomerulonephropathy, and chronic kidney disease (Jin et al., 2019; Sturmlechner, Durik, Sieben, Baker, & van Deursen, 2017), and the present study demonstrates their prominence also in the mouse STK with chronic renal ischemia. The mechanisms underlying cellular senescence in the STK are likely multifactorial. RAS induces renal hypoxia, which can cause cycle arrest in many cell types (Hubbi & Semenza, 2015). Hypoxia-inducible factors contribute to cell cycle arrest through both non-transcriptional effects on the minichromosome maintenance helicase during DNA replication and transcriptional activation of genes encoding the CDK inhibitors *p*21 and *p*27 (Hubbi & Semenza, 2015). Furthermore, HIF-1α-inducible histone lysine demethylases lead to activation of genes in the INK4 box, containing INK4a (*p*16), INK4b (*p*15), and ARF (*p*19), as well as the RB-stimulated tumor suppressor genes, which promote senescence (Salminen, Kaarniranta, & Kauppinen, 2016). Indeed, we observed upregulated HIF-1α, *p*16, *p*21, and *p*53 gene expression in the STK, probably secondary to renal hypoxia. Additional factors that may contribute to STK senescence include reactive oxygen species that may produce DNA damage foci, with a contribution of *p*21 (Passos et al., 2010), and excessive matrix accumulation that promotes senescence in response to angiotensin-II (Yin

& Pickering, 2016). Aldosterone also induces renal senescence in proximal tubular cells *via* a *p*21-dependent pathway (Fan et al., 2011). In addition, disturbed STK flow might promote endothelial senescence *via* a *p*53-dependent pathway (Warboys et al., 2014).

When cells senesce, they adopt a SASP characterized by common set of proteins, including secreted inflammatory cytokines, immune modulators, and growth factors, such as IL-1α, IL-6, IL-8, transforming growth-factor (TGF)-β, and TNF-α (Prattichizzo et al., 2016). Particularly, IL-1α is a key senescence-associated pro-inflammatory cytokine that acts as a critical upstream regulator of SASP (Wiggins et al., 2019). In our previous studies, human and swine STKs had elevated expression of IL-1α, IL-6, TNF-α, and important mediators of irreversible kidney damage and renal fibrosis, which might be related to the SASP (Eirin et al., 2013; Eirin et al., 2014). We found in this study that renal fibrosis was closely related to senescent cell accumulation in the kidney, and Activin-A gene expression was elevated over 200-fold in RAS mice. This member of the TGF superfamily inhibits cell growth and proliferation by stimulating transcription of the cell cycle inhibitors, and may constitute a biomarker of senescent cell burden in diabetes (Bian et al., 2019) and aging. Our observation of increased levels of Activin-A also is therefore consistent with premature STK senescence. Contrarily, Activin-A protein level was similar among the groups; further studies are needed to assess the mechanisms regulating Activin-A gene and protein expression.

MSCs have been as a therapeutic option for STK injury in RAS (Saad et al., 2017). Here, we used both murine and human adipose tissue-derived MSCs, which are relatively abundant and easily accessible (Burrow, Hoyland, & Richardson, 2017). MSCs release growth factors and cytokines, which exert paracrine effects on adjacent cells, inhibiting oxidative stress, inflammation, apoptosis, and fibrosis, and induce new vessel formation (X. Y. Zhu, Lerman, & Lerman, 2013). Pertinently, this study confirms anti-inflammatory, anti-fibrotic, and pro-angiogenic effects of MSCs in the murine STK. We detected labeled MSCs in the mouse kidney after delivery *via* the aorta, consistent with the observation that systemically delivered MSCs home directly to the injured kidney and have beneficial effects (Wise et al., 2014). A recent study, employing twice as many human umbilical cord-derived MSCs delivered intraperitoneally, showed that MSC protect against premature renal senescence in rat AKI (Rodrigues et al., 2017). In our study, IL-6 overexpression was decreased in the STK after MSC delivery, which might indicate a blunted SASP and reduced senescent cell-associated inflammation. However, we did not detect a decrease in IL-1α, TNF-α, *p*16, or *p*21 expression, despite improved renal fibrosis and function. This ostensible discrepancy may be attributable to different mechanisms activated in acute versus chronic ischemia. For example, in swine RAS MSCs prevent STK cellular apoptosis (X. Y. Zhu, Urbieta-Caceres, et al., 2013). Possibly, the anti-apoptotic effect of MSCs might permit survival of some senescent cells and offset long-term improvement of senescence in this study. Nevertheless, MSCs improved renal function (albeit not kidney size), possibly by increasing capillary density and attenuating inflammatory infiltration and fibrosis. Taken together, MSCs had a small impact on gene expression related to senescence, but mitigated some of SASP and its associated inflammation. These findings also imply that cellular senescence has a relatively modest effect on kidney function in chronic ischemia.

Exosomes carry a cargo of molecules that indicate the physiological state of their cells of origin (van Balkom, Pisitkun, Verhaar, & Knepper, 2011). Analysis of RNAs in urinary exosomes benefits from the RNA-protective effect of exosomes, as they include mRNA transcripts encoding specific genes from all regions of the nephron (Miranda et al., 2010). We have recently shown elevated levels of senescence-associated exosomes in urine of hypertensive patients that may reflect increased proximal tubular cellular senescence (Santelli et al., 2019), as levels of senescence markers in urinary exosomes may also reflect those in renal tissue (Zubiri et al., 2015). We have also found that elevated urinary levels of podocyte-derived exosomes and expression of microRNAs in urinary EVs may be linked to renal injury in hypertension (Kwon et al., 2016; Kwon et al., 2017). The current study extends those findings by showing that congruent with findings in the murine STK, *p*21 gene expression and percentage in urinary exosomes is increased in RVH and only partly improved after MSC delivery. Interestingly, *p*16 gene expression was not significantly different among the groups, perhaps because of large variability in HV and RVH. Possibly, *p*21+ urinary exosomes might be a useful noninvasive biomarker of senescence in human subjects.

This study has some notable limitations. Our murine study is limited by small group sizes, relatively young age, shorter duration of RAS than in humans, and high-grade stenosis evident by marked shrinkage of the STK. This atrophy also limits the studies that can be performed on the scant tissue. MSC treatment was not effective in reducing BP and expression of inflammatory cytokines in the STK except for IL-6, possibly because of the severity of the insult, single treatment, and short-term observation. Amelioration of renovascular hypertension in mice may require repeated MSC delivery (Oliveira-Sales et al., 2013), and in humans appears to be dose-dependent (Abumuawad et al., 2020). However, we have previously shown that single delivery of MSCs is effective in improving kidney function and decreasing injury in the swine STK (Eirin et al., 2014), and the dose we used evidently sufficed to normalize renal function. Yet, the *in vivo* fate of transplanted MSCs remains unknown, as do the optimal timing and duration of observation for MSC benefits. The use of allogeneic MSCs could raise concerns about rejection, but syngeneic and allogeneic adipose tissue-derived stem cells seem to have comparable effects (Rezaei & Moazzeni, 2019), arguing against cell rejection. Indeed, we observed no sign of rejection, and the MSCs were clearly effective in improving renal function. In addition, it was challenging to accurately identify the cells positive for SA-β-Gal, which does not easily lend itself to double-staining, although STK renal tubules and glomeruli appeared primarily affected. Finally, the contribution of senescence to renal injury progression remains to be determined. Our Western blot GAPDH bands were thicker in sham than in other groups, possibly because ischemic tissues have lower expression of housekeeping genes (Nie et al., 2017). Our human study was nonrandomized and included a small number of subjects. BMI in patients with RVH was higher than in HV, yet differences between HV and RVH were sustained upon adjustments for BMI. We could not directly determine human STK senescence, because renal tissue was unavailable for analysis. Additionally, technical aspects of exosome isolation and detection remain to be standardized.

In conclusion, our study demonstrates cellular senescence in the murine and human STK, although further studies are needed to determine the role of cellular senescence in kidney

damage in RAS. MSC therapy only partly mitigates renal cell-cycle arrest and senescence activity in RAS, although it ameliorated some of its potential sequelae. Nevertheless, cellular senescence can be blunted using natural flavonoids, food supplements, and senolytic drugs (Hickson et al., 2019; Y. Zhu et al., 2017), which might be more effective than MSCs in long-term amelioration of senescence. Our results thus support novel intervention strategies such as targeted senolytic therapy in RAS to reduce senescent cell burden and delay renal injury.

Supplementary Material

Refer to Web version on PubMed Central for supplementary material.

Acknowledgements

Funding

This work was partly supported by NIH grants numbers DK102325, DK100081, DK104273, DK120292, AG062104, and DK122734. The authors are grateful for support from the Mayo Clinic Histology Core Facility (Arizona) and Pathology Research Core (Rochester, MN).

Conflict of Interest

Dr. Lerman receives grant funding from Novo Nordisk, and is an advisor to Weijian Technologies and AstraZeneca.

References

Abumoawad A, Saad A, Ferguson CM, Eirin A, Herrmann SM, Hickson LJ, Bendel EC, Misra S, Glockner J, Dietz AB, Lerman LO, Textor SC (2020). Autologous mesenchymal stem cell infusion for renovascular disease increases blood flow and GFR while reducing inflammatory biomarkers and blood pressure: A Phase 1a escalating clinical trial. Kidney Int, In press

Bian X, Griffin TP, Zhu X, Islam MN, Conley SM, Eirin A, . . . Hickson LJ (2019). Senescence marker activin A is increased in human diabetic kidney disease: association with kidney function and potential implications for therapy. BMJ Open Diabetes Res Care, 7(1), e000720. doi:10.1136/bmjdrc-2019-000720

Biancone L, Bruno S, Deregibus MC, Tetta C, & Camussi G. (2012). Therapeutic potential of mesenchymal stem cell-derived microvesicles. Nephrology, dialysis, transplantation : official publication of the European Dialysis and Transplant Association - European Renal Association, 27(8), 3037–3042. doi:10.1093/ndt/gfs168

Burrow KL, Hoyland JA, & Richardson SM (2017). Human Adipose-Derived Stem Cells Exhibit Enhanced Proliferative Capacity and Retain Multipotency Longer than Donor-Matched Bone Marrow Mesenchymal Stem Cells during Expansion In Vitro. Stem Cells Int, 2017, 2541275. doi:10.1155/2017/2541275

Chandrasekaran A, Idelchik M, & Melendez JA (2017). Redox control of senescence and age-related disease. Redox Biol, 11, 91–102. doi:10.1016/j.redox.2016.11.005 [PubMed: 27889642]

Ebrahimi B, Crane JA, Knudsen BE, Macura SI, Grande JP, & Lerman LO (2013). Evolution of cardiac and renal impairment detected by high-field cardiovascular magnetic resonance in mice with renal artery stenosis. Journal of cardiovascular magnetic resonance : official journal of the Society for Cardiovascular Magnetic Resonance, 15, 98. doi:10.1186/1532-429X-15-98 [PubMed: 24160179]

Eirin A, Gloviczki ML, Tang H, Gossl M, Jordan KL, Woollard JR, . . . Lerman LO (2013). Inflammatory and injury signals released from the post-stenotic human kidney. European heart journal, 34(7), 540–548a. doi:10.1093/eurheartj/ehs197 [PubMed: 22771675]

Eirin A, Zhang X, Zhu XY, Tang H, Jordan KL, Grande JP, . . . Lerman LO (2014). Renal vein cytokine release as an index of renal parenchymal inflammation in chronic experimental renal artery

stenosis. Nephrology, dialysis, transplantation : official publication of the European Dialysis and Transplant Association - European Renal Association, 29(2), 274–282. doi:10.1093/ndt/gft305

Eirin A, Zhu XY, Ferguson CM, Riester SM, van Wijnen AJ, Lerman A, & Lerman LO (2015). Intra-renal delivery of mesenchymal stem cells attenuates myocardial injury after reversal of hypertension in porcine renovascular disease. Stem cell research & therapy, 6, 7. doi:10.1186/scrt541 [PubMed: 25599803]

Eirin A, Zhu XY, Krier JD, Tang H, Jordan KL, Grande JP, . . . Lerman LO (2012). Adipose tissue-derived mesenchymal stem cells improve revascularization outcomes to restore renal function in swine atherosclerotic renal artery stenosis. Stem cells, 30(5), 1030–1041. doi:10.1002/stem.1047 [PubMed: 22290832]

Eirin A, Zhu XY, Puranik AS, Tang H, McGurren KA, van Wijnen AJ, . . . Lerman LO (2017). Mesenchymal stem cell-derived extracellular vesicles attenuate kidney inflammation. Kidney Int, 92(1), 114–124. doi:10.1016/j.kint.2016.12.023 [PubMed: 28242034]

Ezquer M, Urzua CA, Montecino S, Leal K, Conget P, & Ezquer F. (2016). Intravitreal administration of multipotent mesenchymal stromal cells triggers a cytoprotective microenvironment in the retina of diabetic mice. Stem Cell Res Ther, 7, 42. doi:10.1186/s13287-016-0299-y [PubMed: 26983784]

Fan YY, Kohno M, Hitomi H, Kitada K, Fujisawa Y, Yatabe J, . . . Nakano D. (2011). Aldosterone/Mineralocorticoid receptor stimulation induces cellular senescence in the kidney. Endocrinology, 152(2), 680–688. doi:10.1210/en.2010-0829 [PubMed: 21190955]

Hickson LJ, Langhi Prata LGP, Bobart SA, Evans TK, Giorgadze N, Hashmi SK, . . . Kirkland JL (2019). Senolytics decrease senescent cells in humans: Preliminary report from a clinical trial of Dasatinib plus Quercetin in individuals with diabetic kidney disease. EBioMedicine, 47, 446–456. doi:10.1016/j.ebiom.2019.08.069 [PubMed: 31542391]

Hubbi ME, & Semenza GL (2015). Regulation of cell proliferation by hypoxia-inducible factors. American journal of physiology. Cell physiology, 309(12), C775–782. doi:10.1152/ajpcell.00279.2015 [PubMed: 26491052]

Jin H, Zhang Y, Ding Q, Wang SS, Rastogi P, Dai DF, . . . Attanasio M. (2019). Epithelial innate immunity mediates tubular cell senescence after kidney injury. JCI Insight, 4(2). doi:10.1172/jci.insight.125490

Kim SR, Eirin A, Zhang X, Lerman A, & Lerman LO (2019). Mitochondrial Protection Partly Mitigates Kidney Cellular Senescence in Swine Atherosclerotic Renal Artery Stenosis. Cell Physiol Biochem, 52(3), 617–632. doi:10.33594/000000044 [PubMed: 30907989]

Kwon SH, & Lerman LO (2015). Atherosclerotic renal artery stenosis: current status. Advances in chronic kidney disease, 22(3), 224–231. doi:10.1053/j.ackd.2014.10.004 [PubMed: 25908472]

Kwon SH, Tang H, Saad A, Woollard JR, Lerman A, Textor SC, & Lerman LO (2016). Differential Expression of microRNAs in Urinary Extracellular Vesicles Obtained From Hypertensive Patients. Am J Kidney Dis, 68(2), 331–332. doi:10.1053/j.ajkd.2016.01.027 [PubMed: 26994684]

Kwon SH, Woollard JR, Saad A, Garovic VD, Zand L, Jordan KL, . . . Lerman LO (2017). Elevated urinary podocyte-derived extracellular microvesicles in renovascular hypertensive patients. Nephrology, dialysis, transplantation : official publication of the European Dialysis and Transplant Association - European Renal Association, 32(5), 800–807. doi:10.1093/ndt/gfw077

Miranda KC, Bond DT, McKee M, Skog J, Paunescu TG, Da Silva N, . . . Russo LM (2010). Nucleic acids within urinary exosomes/microvesicles are potential biomarkers for renal disease. Kidney Int, 78(2), 191–199. doi:10.1038/ki.2010.106 [PubMed: 20428099]

Nie X, Li C, Hu S, Xue F, Kang YJ, & Zhang W. (2017). An appropriate loading control for western blot analysis in animal models of myocardial ischemic infarction. Biochem Biophys Rep, 12, 108–113. doi:10.1016/j.bbrep.2017.09.001 [PubMed: 28955798]

Oliveira-Sales EB, Maquigussa E, Semedo P, Pereira LG, Ferreira VM, Camara NO, . . . Boim MA (2013). Mesenchymal stem cells (MSC) prevented the progression of renovascular hypertension, improved renal function and architecture. PLoS One, 8(11), e78464. doi:10.1371/journal.pone.0078464

Passos JF, Nelson G, Wang C, Richter T, Simillion C, Proctor CJ, . . . von Zglinicki T. (2010). Feedback between p21 and reactive oxygen production is necessary for cell senescence. Molecular systems biology, 6, 347. doi:10.1038/msb.2010.5 [PubMed: 20160708]

Pawar AS, Eirin A, Krier JD, Woollard JR, Zhu XY, Lerman A, . . . Lerman LO (2019). Alterations in genetic and protein content of swine adipose tissue-derived mesenchymal stem cells in the metabolic syndrome. Stem Cell Res, 37, 101423. doi:10.1016/j.scr.2019.101423

Prattichizzo F, Giuliani A, Recchioni R, Bonafe M, Marcheselli F, De Carolis S, . . . Olivieri F. (2016). Anti-TNF-alpha treatment modulates SASP and SASP-related microRNAs in endothelial cells and in circulating angiogenic cells. Oncotarget, 7(11), 11945–11958. doi:10.18632/oncotarget.7858 [PubMed: 26943583]

Rezaei F, & Moazzeni SM (2019). Comparison of The Therapeutic Effect of Syngeneic, Allogeneic, and Xenogeneic Adipose Tissue-Derived Mesenchymal Stem Cells on Abortion Rates in A Mouse Model. Cell J, 21(1), 92–98. doi:10.22074/cellj.2019.5954 [PubMed: 30507094]

Rodrigues CE, Capcha JM, de Braganca AC, Sanches TR, Gouveia PQ, de Oliveira PA, . . . Andrade L. (2017). Human umbilical cord-derived mesenchymal stromal cells protect against premature renal senescence resulting from oxidative stress in rats with acute kidney injury. Stem Cell Res Ther, 8(1), 19. doi:10.1186/s13287-017-0475-8 [PubMed: 28129785]

Saad A, Dietz AB, Herrmann SMS, Hickson LJ, Glockner JF, McKusick MA, . . . Textor SC (2017). Autologous Mesenchymal Stem Cells Increase Cortical Perfusion in Renovascular Disease. J Am Soc Nephrol. doi:10.1681/ASN.2017020151

Salminen A, Kaarniranta K, & Kauppinen A. (2016). Hypoxia-Inducible Histone Lysine Demethylases: Impact on the Aging Process and Age-Related Diseases. Aging and disease, 7(2), 180–200. doi:10.14336/AD.2015.0929 [PubMed: 27114850]

Santelli A, Sun IO, Eirin A, Abumoawad AM, Woollard JR, Lerman A, . . . Lerman LO (2019). Senescent Kidney Cells in Hypertensive Patients Release Urinary Extracellular Vesicles. J Am Heart Assoc, 8(11), e012584. doi:10.1161/JAHA.119.012584

Sturmlechner I, Durik M, Sieben CJ, Baker DJ, & van Deursen JM (2017). Cellular senescence in renal ageing and disease. Nat Rev Nephrol, 13(2), 77–89. doi:10.1038/nrneph.2016.183 [PubMed: 28029153]

Sun IO, Santelli A, Abumoawad A, Eirin A, Ferguson CM, Woollard JR, . . . Lerman LO (2018). Loss of Renal Peritubular Capillaries in Hypertensive Patients Is Detectable by Urinary Endothelial Microparticle Levels. Hypertension, 72(5), 1180–1188. doi:10.1161/HYPERTENSIONAHA.118.11766 [PubMed: 30354805]

van Balkom BW, Pisitkun T, Verhaar MC, & Knepper MA (2011). Exosomes and the kidney: prospects for diagnosis and therapy of renal diseases. Kidney Int, 80(11), 1138–1145. doi:10.1038/ki.2011.292 [PubMed: 21881557]

Warboys CM, de Luca A, Amini N, Luong L, Duckles H, Hsiao S, . . . Evans PC (2014). Disturbed flow promotes endothelial senescence via a p53-dependent pathway. Arterioscler Thromb Vasc Biol, 34(5), 985–995. doi:10.1161/ATVBAHA.114.303415 [PubMed: 24651677]

Wiggins KA, Parry AJ, Cassidy LD, Humphry M, Webster SJ, Goodall JC, . . . Clarke MCH (2019). IL-1alpha cleavage by inflammatory caspases of the noncanonical inflammasome controls the senescence-associated secretory phenotype. Aging Cell, 18(3), e12946. doi:10.1111/acel.12946 [PubMed: 30916891]

Wise AF, Williams TM, Kiewiet MB, Payne NL, Siatskas C, Samuel CS, & Ricardo SD (2014). Human mesenchymal stem cells alter macrophage phenotype and promote regeneration via homing to the kidney following ischemia-reperfusion injury. Am J Physiol Renal Physiol, 306(10), F1222–1235. doi:10.1152/ajprenal.00675.2013 [PubMed: 24623144]

Yin H, & Pickering JG (2016). Cellular Senescence and Vascular Disease: Novel Routes to Better Understanding and Therapy. The Canadian journal of cardiology, 32(5), 612–623. doi:10.1016/j.cjca.2016.02.051 [PubMed: 27040096]

Zhu XY, Lerman A, & Lerman LO (2013). Concise review: mesenchymal stem cell treatment for ischemic kidney disease. Stem cells, 31(9), 1731–1736. doi:10.1002/stem.1449 [PubMed: 23766020]

Zhu XY, Urbieta-Caceres V, Krier JD, Textor SC, Lerman A, & Lerman LO (2013). Mesenchymal stem cells and endothelial progenitor cells decrease renal injury in experimental swine renal artery stenosis through different mechanisms. Stem cells, 31(1), 117–125. doi:10.1002/stem.1263 [PubMed: 23097349]

Zhu Y, Armstrong JL, Tchkonia T, & Kirkland JL (2014). Cellular senescence and the senescent secretory phenotype in age-related chronic diseases. Current opinion in clinical nutrition and metabolic care, 17(4), 324–328. doi:10.1097/MCO.0000000000000065 [PubMed: 24848532]

Zhu Y, Doornebal EJ, Pirtskhalava T, Giorgadze N, Wentworth M, Fuhrmann-Stroissnigg H, . . . Kirkland JL (2017). New agents that target senescent cells: the flavone, fisetin, and the BCL-XL inhibitors, A1331852 and A1155463. Aging (Albany NY), 9(3), 955–963. doi:10.18632/aging.101202 [PubMed: 28273655]

Zhu Y, Tchkonia T, Pirtskhalava T, Gower AC, Ding H, Giorgadze N, . . . Kirkland JL (2015). The Achilles' heel of senescent cells: from transcriptome to senolytic drugs. Aging Cell, 14(4), 644–658. doi:10.1111/acel.12344 [PubMed: 25754370]

Zubiri I, Posada-Ayala M, Benito-Martin A, Maroto AS, Martin-Lorenzo M, Cannata-Ortiz P, . . . Alvarez-Llamas G. (2015). Kidney tissue proteomics reveals regucalcin downregulation in response to diabetic nephropathy with reflection in urinary exosomes. Transl Res, 166(5), 474–484 e474. doi:10.1016/j.trsl.2015.05.007

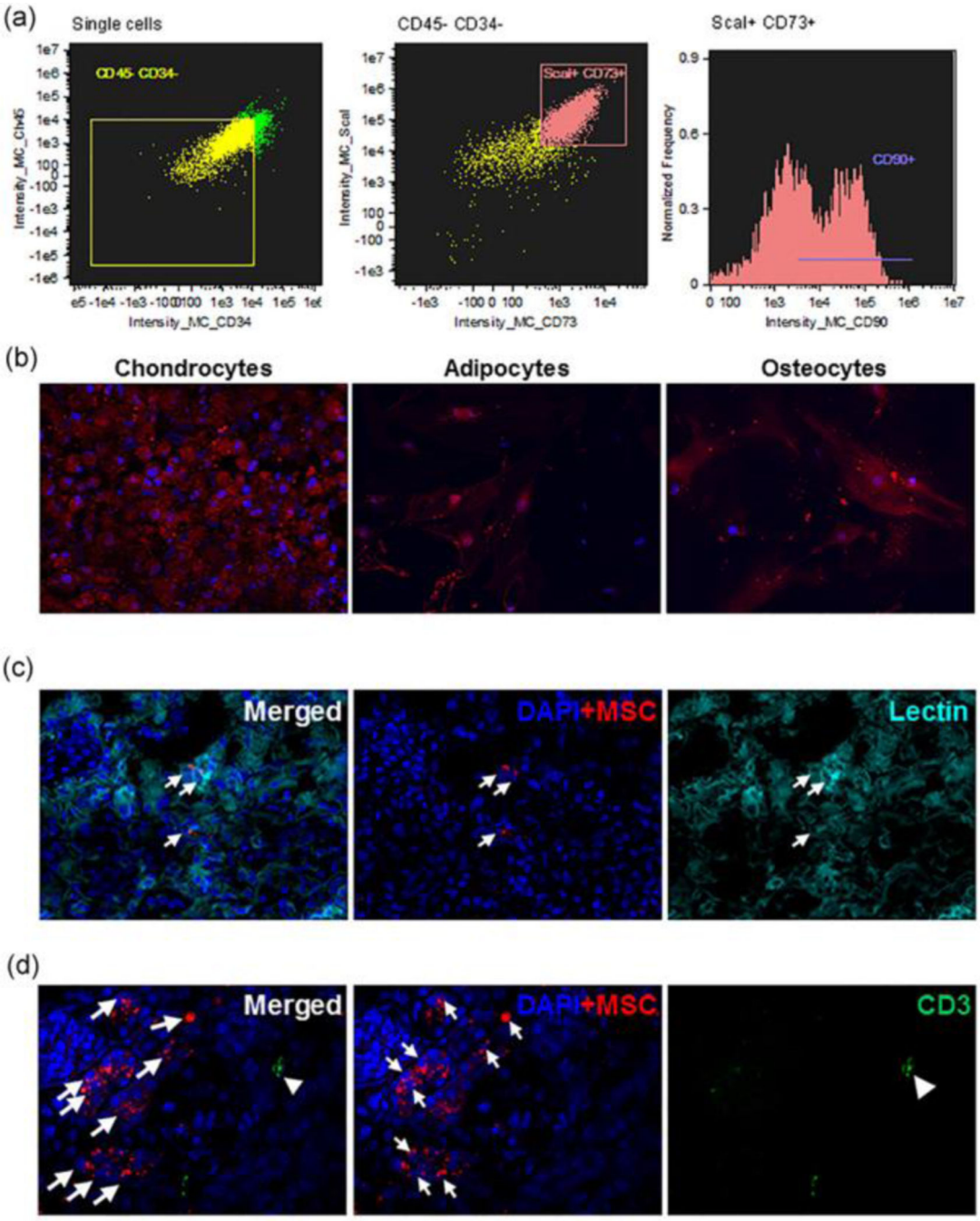

Figure 1.

Characteristics of murine mesenchymal stem cells (MSCs). A. Flow cytometry showed that murine adipose tissue-derived MSCs express Sca-1, CD73, and CD90, but not CD45 or CD34. B. Representative immunofluorescence staining (40X) showing that MSCs trans-differentiated into chondrocytes, adipocytes, and osteocytes *in vitro*, confirming their phenotype. C-D. Representative immunofluorescence (40X) of CM-DiI (red) MSCs in the stenotic-kidney. Most of the allogeneic MSCs (arrow) co-localized with tubular lectin (C),

but not CD3 (arrow head, D), arguing against immune rejection. Lectin: Turquoise, CD3: Green, DAPI: Blue.

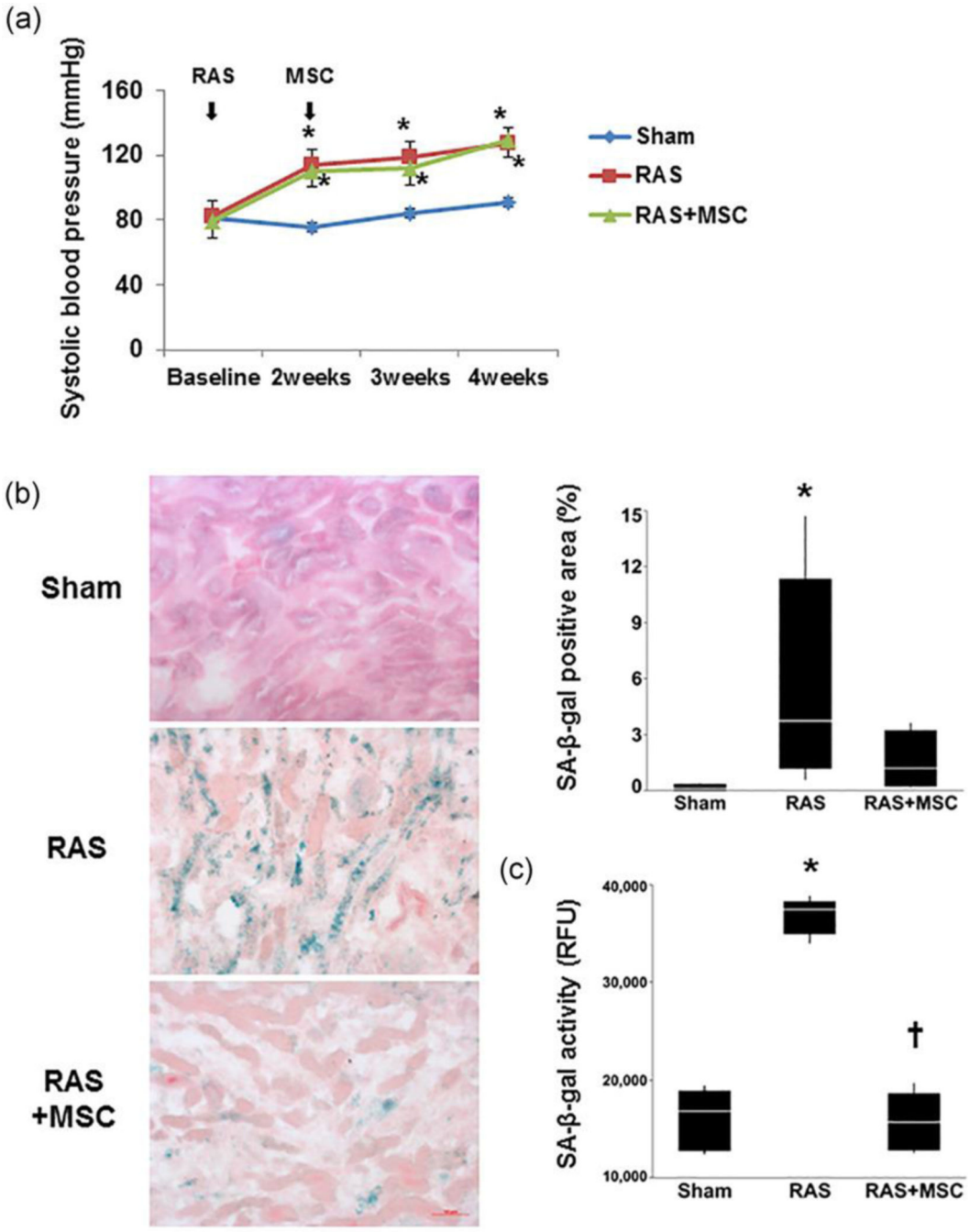

Figure 2.

Blood pressure and renal senescence-associated β-galactosidase (SA-β-Gal) activity. A. Systolic blood pressure in sham, renal artery stenosis (RAS), and RAS+mesenchymal stem cells (MSCs) mice. Systolic blood pressure was similar among the groups at baseline, but rose in both RAS groups starting 2 weeks after RAS induction. *P≤0.05 *vs.* sham and baseline in the same group. B. Representative renal SA-β-Gal staining (20X) in sham, RAS, and RAS+MSC mice. The percentage of SA-β-Gal positive area was higher in the stenotic kidney (STK) of RAS than in sham, but MSC did not significantly affect this compared with

RAS, although RAS+MSC were no longer different that Sham. C. SA-β-Gal activity using fluorometric assay was higher in the STK than in sham, and decreased after MSC delivery. RFU, relative fluorescence units. *P≤0.05 *vs.* sham, †P≤0.05 *vs.* RAS, ††P≤0.001 *vs.* RAS.

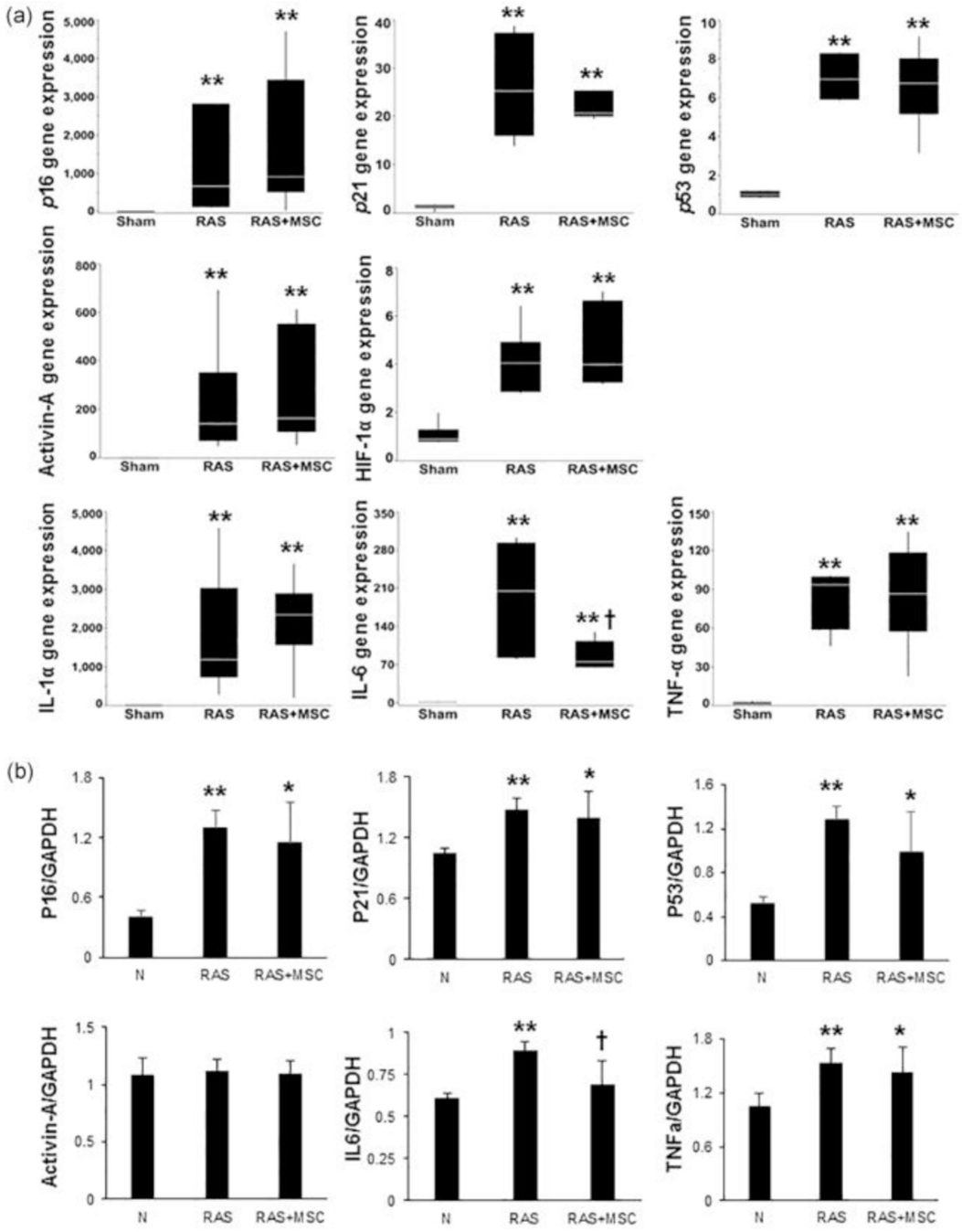

Figure 3.

Cellular senescence-related gene and protein expression. A. Renal *p*16, *p*21, *p*53, Activin-A, HIF-1α, IL-1α, IL-6, and TNF-α gene expression (relative to GAPDH) was elevated in renal artery stenosis (RAS) compared with sham. While most showed no change after mesenchymal stem cell (MSC) delivery, IL-6 decreased with MSC treatment. B. Renal *p*16, *p*21, *p*53, IL-6, and TNF-α protein levels (relative to GAPDH) were higher in RAS than sham. MSC treatment lessened IL-6, but no other proteins. Activin-A protein level was similar among the groups. **P≤0.01 *vs.* sham, †P≤0.05 *vs.* RAS.

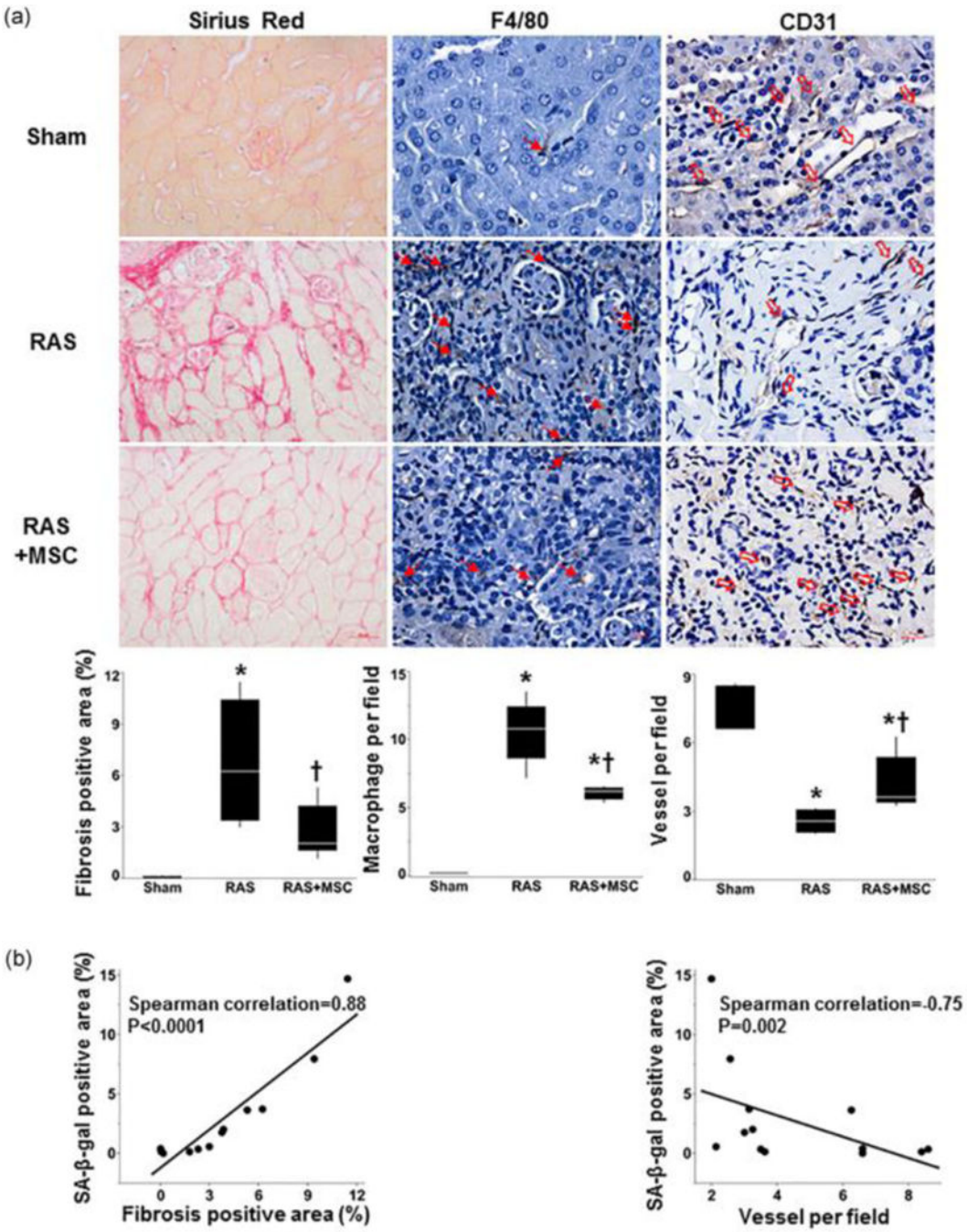

Figure 4.

Fibrosis, inflammatory infiltration, and capillary density in the stenotic kidney. A. Representative renal Sirius red (20X), F40/80 (40X), and CD31 (40X) staining in sham, renal artery stenosis (RAS), and RAS+mesenchymal stem cells (MSCs) mice. Renal collagen deposition and macrophage infiltration (red solid arrow) was higher in RAS and RAS+MSC than in sham, and lower in RAS+MSC than in RAS. RAS showed lower microvascular density (unfilled arrows), which was restored after MSC treatment. B.

Senescence-associated β-galactosidase (SA-β-Gal) positive area correlated directly with renal fibrosis, but inversely with microvascular density. *P≤0.05 *vs.* sham, †P≤0.05 *vs.* RAS.

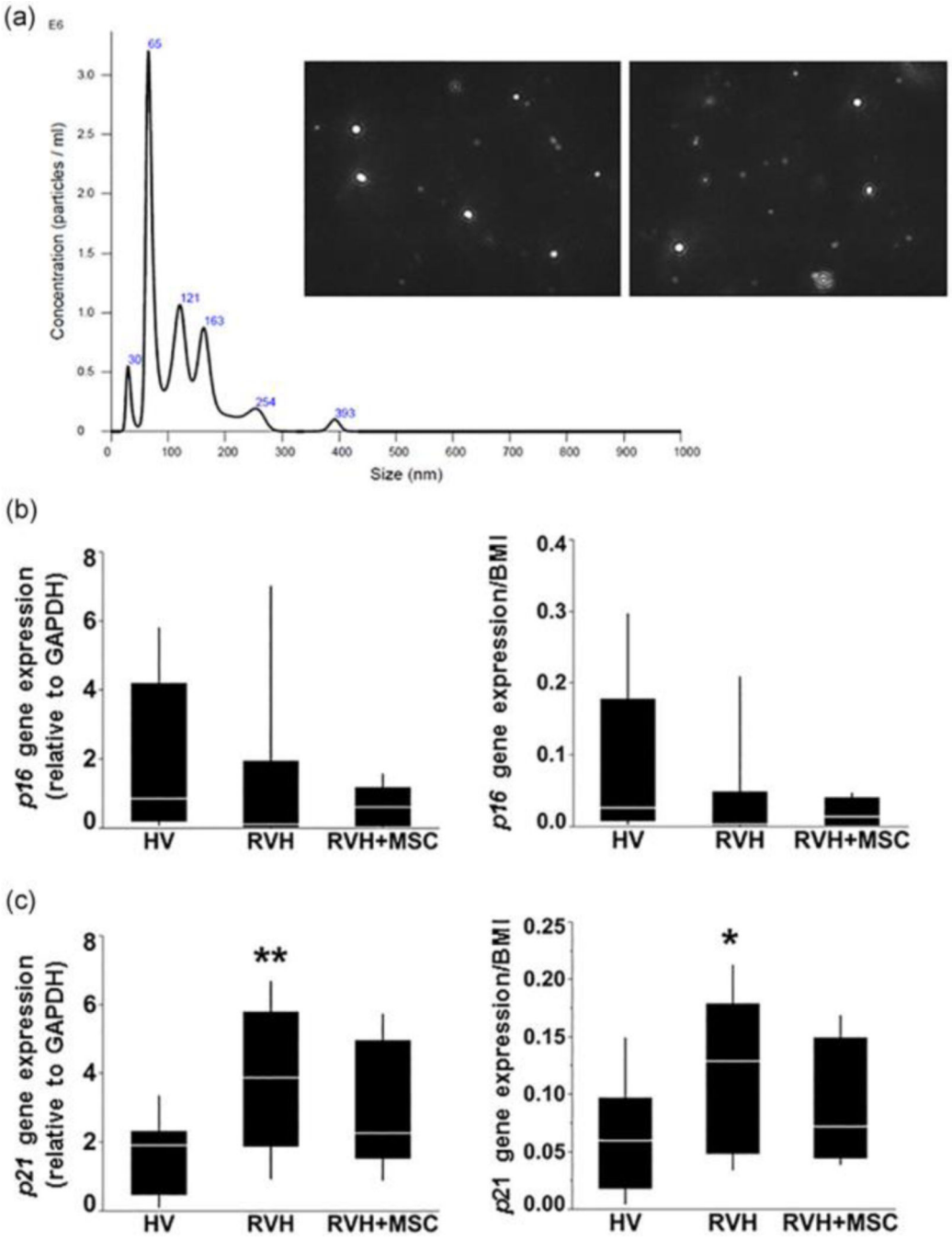

Figure 5.

Characterization and *p*16 and *p*21 gene expression in human urinary exosomes. A. Images and size-distribution of isolated exosomes obtained using NanoSight NS300, showing Over two-thirds 30–100nm in size, consistent with exosomes. B. *p*16 gene expression was not different among the groups, and unaltered after adjustment for BMI. C. *p*21 gene expression was elevated in patients with RVH compared with HV, but not different in patients with RVH+MSC compared with either HV or RVH, even after adjustment for BMI. *P≤0.05, **P≤0.01 *vs.* HV.

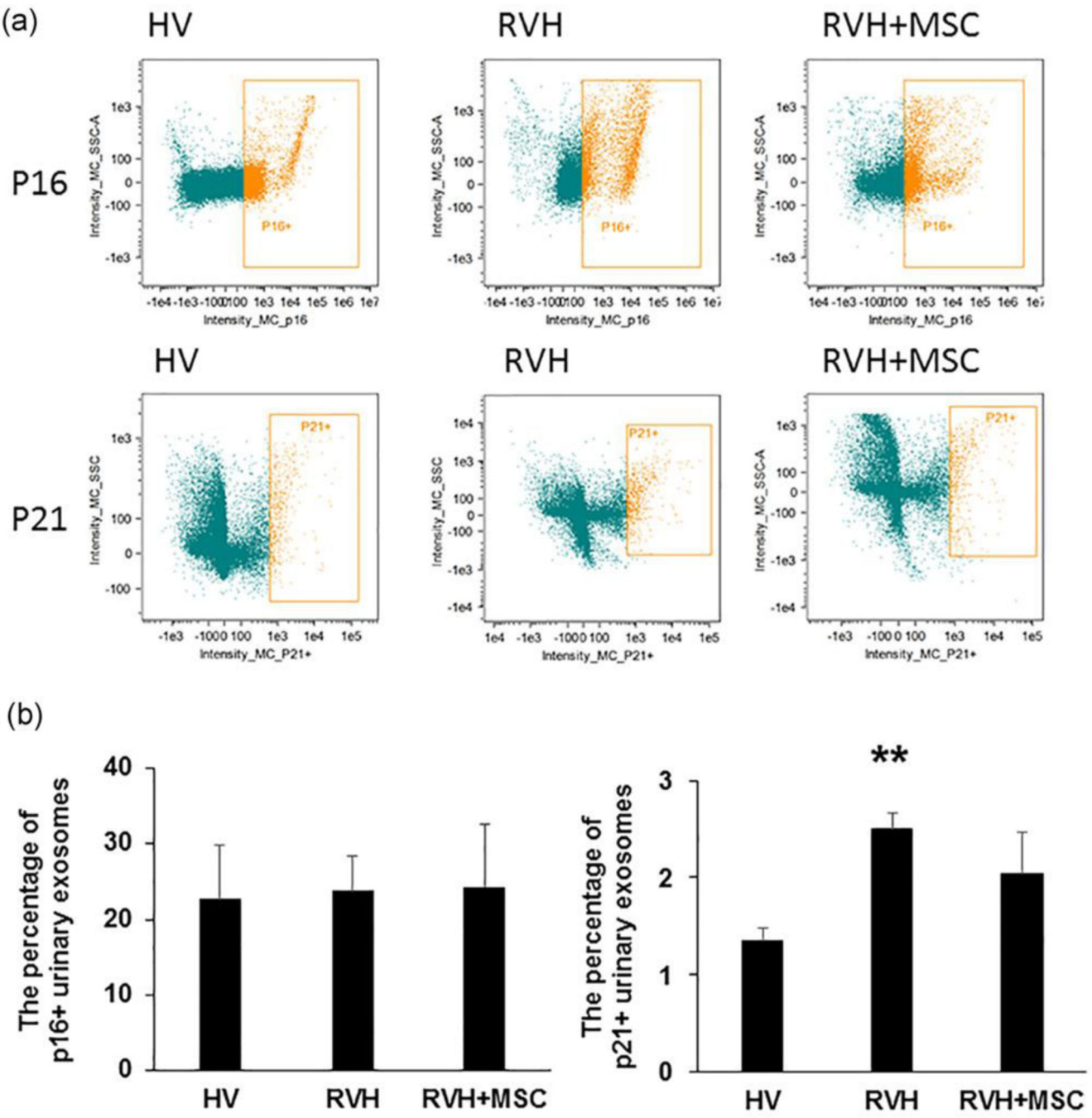

Figure 6.

The percentage of p16+ and p21+ human urinary exosomes using flow cytometry. A. Scatterplots showing samples marked with tag-it-violet and p16 or p21 to identify exosomes from senescent cells. B. In the quantification, p16+ exosomes were unchanged among three groups. Whearas, p21+ exosomes were increased in RVH compared to HV, but no longer higher in RVH+MSC than HV. SSC, side scatter. **P≤0.01 *vs.* HV.

Table 1.

Characteristics of mice 4 weeks after induction of renal artery stenosis (RAS) and injection of mesenchymal stem cells (MSCs)

	Sham (n=6)	RAS (n=6)	RAS+MSC (n=6)
Body weight (g)	24.6±1.05	19.2±2.95 **	22.03±1.88
Kidney weight (mg):			
Stenotic (STK)	206.67±28.87	59.5±4.36 **††	68.67±14.95 **††
Contralateral (CLK)	202.0±24.33	197.0±11.79	237.67±24.34‡
STK/CLK ratio	1.02±0.02	0.30±0.03 **	0.29±0.06 **
Plasma creatinine (mg/dL)	0.16±0.02	0.22±0.02 **	0.16±0.04‡

Data are mean±SD

** P≤0.01 *vs.* sham

†† P≤0.01 *vs.* same-group CLK

‡ P≤0.05 *vs.* RAS

Table 2.

Characteristics of healthy volunteers (HV) and renovascular hypertensive patients (RVH) with and without mesenchymal stem cells (MSCs) delivery 3 months earlier

	HV (n=13)	RVH (n=13)	RVH+MSC (n=6)
Age (y)	73 (67–77.5)	73 (66.5–74.5)	74.5 (71–77)
Sex (men:women)	6:7	7:6	3:3
Body mass index (kg/m^2)	25.7 (22.2–30.8)	31.3 (27.3–35.4) *	30.9 (24.5–36.5)
Arterial blood pressure (mmHg):			
Systolic	122 (115–129.5)	140 (136–153.7) **	133.5 (122.2–136) †
Diastolic	71 (62.5–73.5)	74 (65.5–78)	66.5 (59.5–75.7)
Mean	87.3 (82–92)	96.5 (89.6–104.6) **	89.5 (81.5–94.1)
Serum creatinine (mg/dL)	1.0 (0.8–1.1)	1.4 (1–1.6) **	1.15 (0.9–1.5)
Estimated GFR (ml/min/1.73m^2)	76.5 (71.8–87.7)	45 (39.5–65) **	50.5 (43.2–78) *

Data are medians (interquartile range).

* P≤0.05 *vs.* HV

** P≤0.01 *vs.* HV

† P≤0.05 *vs.* RVH. GFR, glomerular filtration rate